

Mechanical Squeezing via Detuning-Switched Driving

Yaohua Li¹, An-Ning Xu¹, Long-Gang Huang¹, and Yong-Chun Liu^{1,2*}

¹*State Key Laboratory of Low-Dimensional Quantum Physics,*

Department of Physics, Tsinghua University, Beijing 100084, P. R. China and

²*Frontier Science Center for Quantum Information, Beijing 100084, P. R. China*

(Dated: March 9, 2023)

Generation of mechanical squeezing has attracted a lot of interest for its nonclassical properties, applications in quantum information, and high-sensitivity measurement. Here we propose a detuning-switched method that can rapidly generate strong and stationary mechanical squeezing. The pulsed driving can dynamically transpose the optomechanical coupling into a linear optical force and maintain an effective mechanical frequency, which can introduce strong mechanical squeezing in a short time. Moreover, we show the obtained strong mechanical squeezing can be frozen by increasing the pulse intervals, leading to stationary mechanical squeezing with a fixed squeezing angle. Thus, our proposal provides fascinating insights and applications of modulated optomechanical systems.

I. INTRODUCTION

Mechanical squeezed states allow the quantum fluctuation of a single quadrature below the zero-point fluctuation. The unavoidable fluctuations limit the precision of measurement of mechanical quadratures, which then can be surpassed with the mechanical squeezed states [1, 2]. Mechanical squeezing was firstly considered and realized in the parametric resonators [3, 4], the frequency of which was modulated at twice the original mechanical oscillation frequency. In optomechanical systems, the parametric squeezing can be realized by the modulation of the optical spring [5–9]. However, the steady-state squeezing degree is limited to 3dB due to the divergence of the amplified quadrature [4]. To obtain strong mechanical squeezing, additional measurement and appropriate feedback control are required to suppress the amplification [9–12]. Conversely, measurements can also be used to prepare quantum states, especially the mechanical squeezed states [13–16]. With sufficiently strong measurements and optimal estimation of the quadrature, strong mechanical squeezing can be obtained in a conditional state [17, 18]. However, feedback force related to the estimation results is also required to convert the system into unconditional squeezing [19–21].

Instead of a long dissipative evolution, strong mechanical squeezing can be also obtained in nonequilibrium processes, for example, via the rapid [22–25], periodic [26–28] or pulsed [29, 30] modulations of the optical driving, and through the unstable multimode dynamics [31]. Different designs of optical driving structures can touch different goals, including ultra-precise measurements and state preparation, without other assistance or additional feedback. State preparation with fast pulses has made great progress in the experiment [32, 33]. However, the amplitude-modulated structure requires the cavity decay rate much larger than the mechanical frequency to

keep the pulse durations small after inputting the cavity [34, 35], which precludes further squeezing of the mechanical mode. Moreover, the mechanical squeezing obtained from nonequilibrium processes is far from a steady state, and the rapid preparation of stationary mechanical squeezing remains a challenge.

In this work, we firstly analyze the squeezing effect of a mechanical resonator induced by the detuning-switched driving in an optomechanical system [see Fig. 1]. A series of four optical rotating pulses, which introduce an additional small period to the optical mode, yield quick measurements of mechanical position and induce a linear optical force. We can directly control the effective mechanical frequency and obtain pure squeezing terms through the optical force. Without additional readout and feedback control, the mechanical mode evolves to a deterministic squeezed state in a short time under the pulsed driving. By increasing the pulse interval, we further increase or decrease the effective mechanical frequency. In this way, the squeezed state becomes a thermal coherent state of the mechanical resonator under effective frequency, and we obtain stationary mechanical squeezing without a long dissipative evolution. Stationary mechanical squeezing allows improved measurement precision of a fixed quadrature, which is not available with conditional or rotated squeezing states.

II. SYSTEM MODEL

In the rotating frame with the frequency of the driving laser, such an optomechanical model can be well described by the Hamiltonian as $H = -\Delta(t)a^\dagger a + \omega_m b^\dagger b + ga^\dagger a(b + b^\dagger) + \Omega a^\dagger + \Omega^* a$, where a (a^\dagger) and b (b^\dagger) are the optical and mechanical annihilation (creation) operator. ω_m is the mechanical resonance frequency. g is the single-photon optomechanical coupling strength. Ω describes the laser driving strength and $\Delta(t)$ is the time-dependent detuning between the driving laser and cavity resonance frequency. The optical (mechanical) decay rate is κ (γ). Most of the time, $\Delta(t) = \Delta_0$ keeps a small value

* ycliu@tsinghua.edu.cn

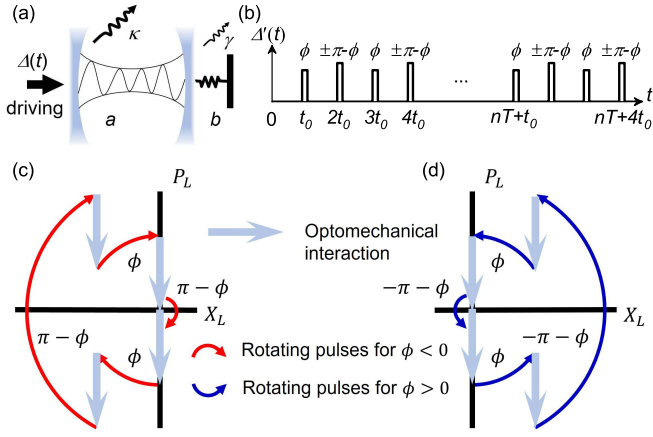


FIG. 1. Optomechanical model with detuned-switched driving. (a) Schematic of the optomechanical model in this work. The cavity mode is driven by a detuning-switched laser. (b) The detuning structure as a function of time with $\phi \in [-\pi, \pi]$. A series of four optical rotating pulses are applied to the optical mode through large detunings. (c),(d) Sketches of the evolution of optical quadrature operators in a four-pulse period for $\phi < 0$ (c) and $\phi > 0$ (d). The straight arrows and curved arrows indicate the evolutions between and during rotating pulses.

(compared with the enhanced optomechanical coupling strength G) except during the rotating pulse when the detuning is shifted to a huge value to rapidly change the relative phase of the cavity field. As the rotating pulse is very short (compared with the pulse interval), we can still employ the linearized process, i.e., $a \rightarrow a + \alpha$ and $b \rightarrow b + \beta$ where $\alpha = \langle a \rangle$ and $\beta = \langle b \rangle$ are the average amplitudes of the optical and mechanical mode. Then the linearized Hamiltonian can be obtained as (see Appendix A for more details)

$$H_L = -\Delta'(t)a^\dagger a + \omega_m b^\dagger b + (Ga^\dagger + G^*a)(b + b^\dagger), \quad (1)$$

where $\Delta'(t) = \Delta(t) - g(\beta + \beta^*)$ is the effective detuning and $G = g\alpha$ is the enhanced optomechanical coupling strength.

The detuning during each pulse is so large that the evolution of the mechanical resonator and optomechanical coupling can be neglected. Then the evolution can be described by the rotating operators $R(\theta_j) = e^{i\theta_j a^\dagger a}$, where $\theta_j = \int_{jt_0}^{j t_0 + \delta t} \Delta'(\tau) d\tau$ is the rotating angle during each pulse and $\theta_j = \phi, \pm\pi - \phi, \phi, \pm\pi - \phi, \dots$ ($\phi \in [-\pi, \pi]$) in our pulse structure [see Fig. 1(b)]. As shown in Fig. 1(c) and 1(d), the first two evolutions between rotating pulses in a four-pulse period yield quick measurement and store the information in quadrature P_L which then be erased and renewed soon within the rotating pulses [see Fig. 1(c) and 1(d)]. The rotating pulses also transpose the information to quadrature X_L which can react on the mechanical quadratures soon in the later optomechanical coupling. The information transposed by pulses

with rotating angles $\phi > 0$ [see. Fig. 1(c)] and $\phi < 0$ [see. Fig. 1(d)] is different, which results in opposite feedback controls of the mechanical quadratures. These two sketches are plotted according to the Heisenberg equations [see Eq. (9) and (10) in the following]. We note that the cavity quadratures will not rotate following the driving laser if we only employ a sudden switch of the laser frequency. It also requires a stronger power of the driving laser to compensate for the larger detuning, and the phase of the laser driving should also be adjusted. Moreover, the detuning should not be enlarged arbitrarily fast, but in a time scale smaller than the round trip time of the cavity. In this case, the cavity can still reach a new equilibrium with the large detuning [see Appendix F for more details].

It's convenient to employ the Baker-Campbell-Hausdorff formula here to analyze the whole evolution operator in a four-pulse period (the total rotating phase of the optical field in a period is 2π), which can be written as

$$U(T) = [R(\pi - \phi)U(t_0)R(\phi)U(t_0)]^2, \quad (2)$$

where $T = 4t_0$ is the four-pulse period and $U(t_0) = e^{-iH_L t_0}$ describes the evolution between two pulses. The effective detuning between two pulses is $\Delta_0 - g(\beta + \beta^*) \equiv \Delta'_0$. Here we employ an approximation that the pulse interval is small, i.e., $\omega_m t_0 \ll 1$. Then the higher order terms in the BCH formula can be directly neglected except for the first and second ones, leading to a Hamiltonian that satisfies $U(T) = e^{-iH_0 T}$. The Hamiltonian can be written as $H_0 = H_{\text{eff}} + H'$, where

$$H_{\text{eff}} = \omega_m b^\dagger b + \sigma(b + b^\dagger)^2, \quad (3)$$

$$\sigma = \frac{1}{2}|G|^2 t_0 \sin\phi, \quad (4)$$

and $H' = -\Delta'_0 a^\dagger a + \Delta'_0(\mu a^\dagger + \mu^* a)(b + b^\dagger) + \omega_m(\mu a^\dagger - \mu^* a)(b - b^\dagger)$, $\mu = \frac{1}{4}Gt_0(1 + e^{i\phi})$ (see Appendix B for more details). In the strong coupling and small detuning regime that we consider, i.e., $|G\sin\phi| \gg |\Delta'_0|, \omega_m$, and with the assumption that $|\mu| \ll 1$, the last two optomechanical coupling terms of H' can be neglected. Thus the first term of H' can be neglected together, leaving an effective Hamiltonian that contains pure mechanical squeezing terms $b^2 + b^{\dagger 2}$ without any optomechanical couplings.

III. SQUEEZING GENERATION.

To understand and quantify the obtained mechanical squeezing, we further introduce dimensionless quadratures defined as $X_L = a + a^\dagger$, $P_L = i(a^\dagger - a)$, $X_M = b + b^\dagger$, $P_M = i(b^\dagger - b)$ and $Y_M = be^{-i\theta/2} + b^\dagger e^{i\theta/2}$, where Y_M is the squeezed mechanical quadrature and θ is the squeezing angle. So the Hamiltonian in Eq. (B6) can be rewritten as $H_{\text{eff}} + 1/2 = \omega_m(X_M^2 + P_M^2)/4 + \sigma X_M^2$. It means

that the optomechanical coupling can be dynamically transposed into a constant modulation of the potential energy or the spring constant felt by the mechanical resonator. In other words, such pulse structure can rapidly maintain an effective mechanical resonance frequency as

$$\omega_s = \sqrt{\omega_m(\omega_m + 4\sigma)}, \quad (5)$$

in the dynamically stable regime for $\sigma > -\omega_m/4$. $\sigma = -\omega_m/4$ is the threshold condition of the pulsed driving. When above the threshold, the variance of amplified mechanical quadrature increases exponentially. Noted that the threshold only exists when the rotating angle $\phi < 0$ when the effective potential energy of the mechanical resonator is reduced to zero.

It is more clear from the Heisenberg equations of quadratures. Without losing generality, we assume G was real. Then the linear Hamiltonian in Eq. (1) can be rewritten as

$$H_L = -\frac{1}{4}\Delta'(t)(X_L^2 + P_L^2) + \frac{1}{4}\omega_m(X_M^2 + P_M^2) + GX_LX_M, \quad (6)$$

and the Heisenberg equations are given by

$$\dot{X}_L = -\Delta'(t)P_L, \quad \dot{P}_L = \Delta'(t)X_L - 2GX_M, \quad (7)$$

$$\dot{X}_M = \omega_m P_M, \quad \dot{P}_M = -\omega_m X_M - 2GX_L. \quad (8)$$

Between two pulses, we have $\Delta'(t) = \Delta'_0 \ll G$. Eq. (7) can be reduced to

$$\dot{X}_L \approx 0, \quad \dot{P}_L \approx -2GX_M. \quad (9)$$

And during the pulses, $\Delta'(t) \gg G$, we have

$$\dot{X}_L \approx -\Delta'(t)P_L, \quad \dot{P}_L \approx \Delta'(t)X_L. \quad (10)$$

Fig. 1(c), and 1(d) are plotted according to Eq. (9) and (10). As shown in Eq. (9), the optomechanical coupling between two nearest pulses generates a measurement on the mechanical quadrature X_M . Then the rotating pulse transposes the information into another optical quadrature X_L and changes the optical force. The average optical force can be obtained as

$$F_{\text{ave}} = -\sigma X_M. \quad (11)$$

which is proportional to the mechanical quadrature X_M . If $\phi = 0, \pm\pi$, the average optical force is zero with no squeezing effect. There are similar quick measurements, but the information is only stored in P_L and does not react on the mechanical quadratures. If $\phi = \pm\pi/2$, the information is transposed totally and maximal squeezing degree can be obtained.

As an example for $\phi = \pi/2$, we plot the detailed Wigner functions and the evolution of quadrature variances in the first four-pulse period, starting with both optical and mechanical modes vacuum states [see Fig. 2 and Appendix C]. Without the pulses, the optomechanical coupling, as called X-X coupling, will generate large

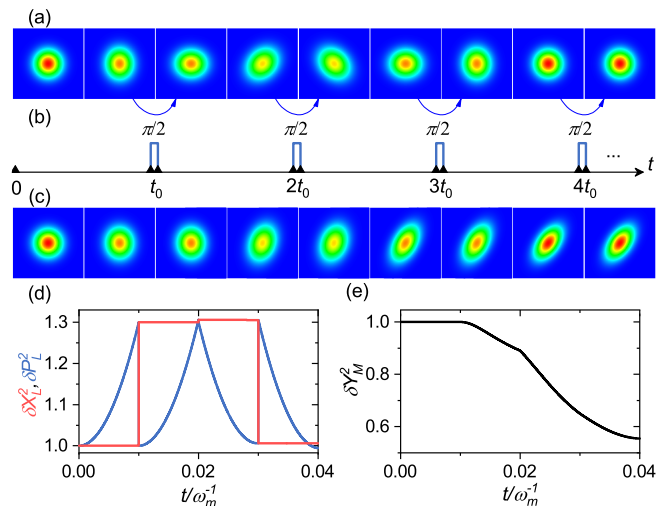


FIG. 2. Generation of mechanical squeezing. (a),(c) The Wigner functions of the optical (a) and mechanical (c) modes at certain times labeled in (b) by black triangles. The vertical axis is X_i and the horizontal axis is P_i for $i = L, M$. (b) The detailed detuning structure in the first four-pulse period, corresponding to $\phi = \pi/2$ in Fig. 1(b). (d),(e) The time evolutions of optical (d) and mechanical (e) quadrature variances. The initial photon and phonon numbers are both zero. Other parameters are $\omega_m t_0 = 0.01$, $\omega_s = 4\omega_m$, $\Delta'_0 = 0$,

amplification of optical quadrature P_L due to large optomechanical coupling strength. Additional pulses turn the trend around and, at the same time, transpose the information from P_L to X_L . The latter can react to the mechanical quadratures, leading to a linear optical force and an effective mechanical frequency. Moreover, after the four-pulse sequence, all the mechanical information written on the optical field is erased, and the mechanical quadratures are correlated. It means that the mechanical squeezing obtained is very pure without measurement.

IV. STATIONARY MECHANICAL SQUEEZING

As the pulsed driving rapidly maintains an effective mechanical frequency ω_s , the mechanical quadratures will rotate with the frequency, accompanied by quadrature squeezing with periodically changed squeezing degree and squeezing angle. The approximate time evolution of mechanical quadratures can be derived from the effective Hamiltonian H_{eff} and corresponding master equations. For $\sigma > -\omega_m/4$ below the threshold, the evolution of variance of squeezed mechanical quadrature is given by

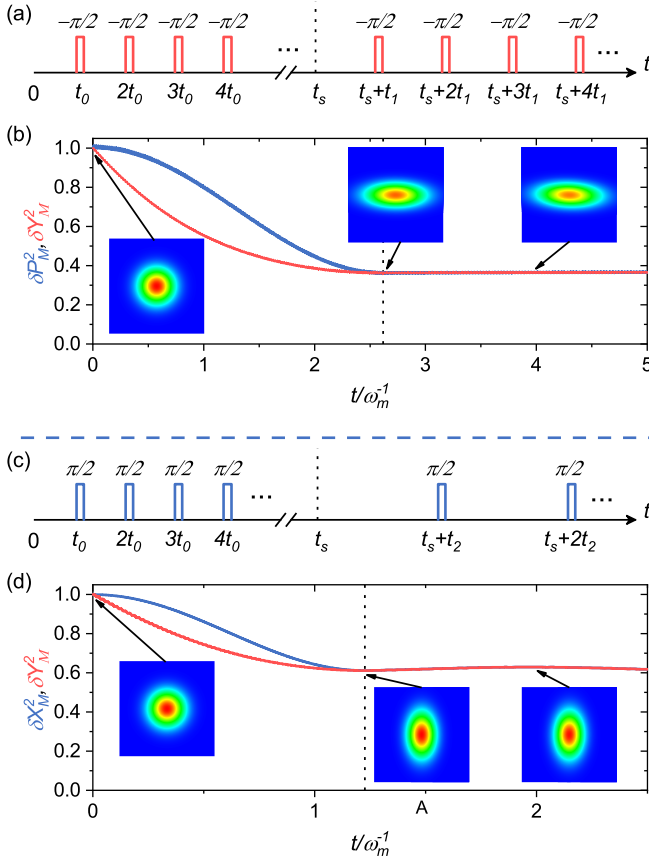


FIG. 3. Stationary mechanical squeezing. (a),(b) $\phi = -\pi/2$, (c),(d) $\phi = \pi/2$. (a),(c) The detuning structures to realize stationary mechanical squeezing. The pulse interval is increased to $t_{1,2}$ after obtaining maximum squeezing degree, i.e., $t = t_s$. (b),(d) The time evolutions of mechanical quadrature variances for $\omega_m t_0 = 0.005$ and $G/\omega_m = 8$. The insert figures are Wigner functions of mechanical mode at three certain times denoted by the arrows. Other unspecified parameters are the same as in Fig. 2.

(see Appendix D for more details)

$$\delta Y_M^2(t) = (1 + 2n_{\text{th}}) \left[1 - \frac{2\sigma^2}{\omega_s^2} \cos^2 \omega_s t \left(\sqrt{1 + \frac{\omega_s^2}{\sigma^2 \cos^2 \omega_s t}} - 1 \right) \right], \quad (12)$$

where n_{th} is the phonon number of the initial mechanical state. We have neglected the mechanical decay rate, as we are only interested in the short-time evolution far from equilibrium. The maximal squeezing degree is obtained at half the evolution period, i.e.,

$$t_s = \frac{\pi}{2\omega_s}. \quad (13)$$

And the minimal variances of squeezed quadrature are approximately given by

$$(\delta Y_M^2)_{\min} = \begin{cases} (1 + 2n_{\text{th}}) \frac{\omega_m + 4\sigma}{\omega_m}, & -\frac{\omega_m}{4} < \sigma < 0 \\ (1 + 2n_{\text{th}}) \frac{\omega_m}{\omega_m + 4\sigma}. & \sigma > 0 \end{cases} \quad (14)$$

The initial phonon number can be very low ($n_{\text{th}} \lesssim 1$) as we can employ laser cooling before the generation of mechanical squeezing. It means that our proposal can squeeze a mechanical mode with quadrature variance far below the zero-point fluctuation.

The maximally squeezed state at $t = t_s$ is a thermal coherent state of the mechanical resonator with another frequency, $\omega'_s = \omega_m + 4\sigma$. The effective Hamiltonians with these two frequencies are given by

$$H_{\text{eff}} = \frac{1}{4} \omega_s \left(\sqrt{\frac{\omega_m + 4\sigma}{\omega_m}} X_M^2 + \sqrt{\frac{\omega_m}{\omega_m + 4\sigma}} P_M^2 \right) - \frac{1}{2} \quad (15)$$

$$H_{\text{eff}} = \frac{1}{4} \omega'_s \left(X_M^2 + \frac{\omega_m}{\omega_m + 4\sigma} P_M^2 \right) - \frac{1}{2} \quad (16)$$

The mechanical quadratures with frequency ω'_s is unsqueezed at $t = t_s$, i.e. $(\omega_m + 4\sigma)\delta X_M^2 = \omega_m \delta P_M^2$. It means that the squeezed state is a thermal state with the effective frequency ω'_s and its Wigner function is a circle. The thermal state will be kept in the later evolution. Consequently, if we increase the pulse interval for $t > t_s$ and thus change the effective mechanical frequency to ω'_s , the mechanical mode will keep stationary at the maximally squeezed state, with both the squeezing degree and the squeezing angle unchanged. The idea of generating stationary squeezing by changing the frequency is firstly proposed by Ref. [36]. Here we can realize it by increasing the pulse interval. The increased pulse intervals are

$$t' = 2t_0 \left[1 + \frac{|G|^2 t_0}{\omega_m} \sin \phi \right]. \quad (17)$$

The detailed pulse structures are shown in Fig. 3(a) and 3(c), where t_1 (t_2) is the increased pulse interval for $\phi = -\pi/2$ ($\pi/2$). In Fig. 3(b) and 3(d), we plot the time evolutions of mechanical quadratures in the two cases. The mechanical mode evolves to the maximally squeezed state at $t = t_s$. Afterward, we increase the pulse interval and obtain stationary mechanical squeezing in a short time. In particular, mechanical quadrature P_M is squeezed ($Y_M = P_M$) with a squeezing angle $\theta = \pi$ for $\phi < 0$, while for $\phi > 0$ the squeezed mechanical quadrature is $Y_M = X_M$ with a squeezing angle $\theta = 0$.

V. SQUEEZING PERFORMANCE

To verify the accuracy of the approximations made in the derivation of effective Hamiltonian, we plot the minimal variance of squeezed quadrature Y_M as a function of

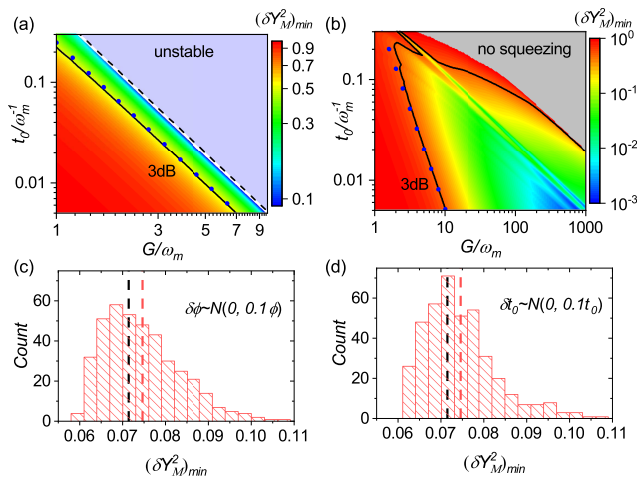


FIG. 4. Influence of parameters and Gaussian errors. (a),(b) The minimal variance of Y_M as a function of G and t_0 for $\phi = -\pi/2$ (a) and $\phi = \pi/2$ (b). The black solid line (blue dots line) indicates the contour line for 3dB squeezing of numerical (analytical) results. The light blue (grey) shadow indicates the unstable (no-squeezing) region. (c),(d) The histogram of minimal variances of Y_M in 400 calculation events when adding Gaussian error to either rotating angles (c) or pulse intervals (d) of each pulse. The standard deviations of Gaussian errors are both one-tenth of the average values, which is $\phi = \pi/2$ and $t_0 = 0.01\omega_m^{-1}$. The average results are $(\delta Y_M^2)_{\min} = 0.0746$ (red dashed line in panel (c)) and $(\delta Y_M^2)_{\min} = 0.0745$ [red dashed line in panel (d)]. Without the Gauss error, the minimal variance is $(\delta Y_M^2)_{\min} = 0.0714$ (black dashed line in panels (c) and (d)). Other parameters are $\Delta_0^2 = 0$, $\omega_s = 4\omega_m$, i.e. $G \approx 27.4\omega_m$.

G and t_0 for $\phi = -\pi/2$ [see Fig. 4(a)] and $\phi = \pi/2$ [see Fig. 4(b)]. Large squeezing degrees can be obtained in a wide range of parameters, as predicted by Eq. (C12). But the approach works badly with parameters away from our assumptions ($\omega_m t_0 \ll 1$, $G \gg \omega_m$ and $|\mu| \ll 1$, i.e., $|Gt_0| \ll 1$). When $|Gt_0| \gtrsim 1$, the optomechanical coupling terms that we used to neglect will greatly influence the evolution of mechanical mode and reduce the squeezing degree. For $\phi < 0$, the parameter region $|Gt_0| \gtrsim 1$ is deep into the unstable region which we are not interested in. To be clear, we emphasize the contour line of 3dB squeezing (black solid lines), which agrees well with the exact values (blue dot lines) for appropriate parameters.

Furthermore, in Fig. 4(c) and 4(d), we analyze the influence of Gaussian errors that may exist in the parameters of pulse structure, i.e. ϕ and t_0 . Typical Gaussian errors result in a variance of squeezing degrees with similar scaling compared with the average value. The average value of minimal variance is larger than the exact result without Gaussian error.

VI. CONCLUSION

In conclusion, we propose a detuning-switched scheme that can dynamically generate strong and stationary mechanical squeezing in the optomechanical system rapidly. The detuning-switched pulses can transpose the optomechanical coupling into a linear optical force felt by the resonator and maintain an effective mechanical frequency, leading to a pure squeezing term. The squeezing process originates from a series of single-quadrature measurements and feedback through the optomechanical interactions, while the large-detuning pulses rotate the optical quadratures and allow the information of mechanical quadrature to be transferred, erased, and renewed in the optical quadratures. With this method, a large amount of squeezing can be achieved rapidly without a long dissipative evolution. Moreover, we show the squeezing degree and the squeezing angle at the maximally squeezed state can be frozen by increasing the pulse interval, i.e., further increasing or reducing the effective mechanical frequency. This method works well with large-range parameters and is robust to the Gaussian-shape error of pulse areas and pulse intervals. Our pulsed scheme can be also applied to other bosonic models that have a similar form of coupling, which provides a unique method to generate stationary squeezing in these systems.

ACKNOWLEDGMENTS

We are extremely grateful to the anonymous referees for their insightful comments on a better understanding of our scheme (e.g., discussions in Appendix F). This work is supported by the Key-Area Research and Development Program of Guangdong Province (Grant No. 2019B030330001), the National Natural Science Foundation of China (NSFC) (Grants No. 12275145, 92050110, 91736106, 11674390, and 91836302), and the National Key R&D Program of China (Grants No. 2018YFA0306504).

Appendix A: System Hamiltonian

We consider a common optomechanical model that a Fabry-Perot cavity with cavity mode a and frequency ω_c is coupled with a mechanical oscillator with mechanical mode b and frequency ω_m . To dynamically generate mechanical squeezing, a series of four optical rotating pulses with equal interval t_0 are included by rapidly changing the frequency of the driving laser, i.e. the detuning. The system Hamiltonian can be written as

$$H_S = \omega_c a^\dagger a + \omega_m b^\dagger b + g a^\dagger a (b + b^\dagger) + (\Omega e^{-i\omega_L(t)t} a^\dagger + \text{H.c.}), \quad (\text{A1})$$

where g is the single-photon optomechanical coupling strength and Ω [$\omega_L(t)$] is the strength [frequency] of the optical driving. In the rotating frame with frequency

$\omega_L(t)$, the Hamiltonian can be rewritten as

$$H = -\Delta(t)a^\dagger a + \omega_m b^\dagger b + ga^\dagger a(b + b^\dagger) + (\Omega a^\dagger + \text{H.c.}), \quad (\text{A2})$$

where $\Delta(t) = \omega_L(t) - \omega_c$ is the laser detuning. We note here we have neglected the term containing the time derivative of the laser frequency, which is nonzero at the beginning and the end of the large-detuning pulses. Because this term will cancel each other at the beginning and the end of the large-detuning pulses as the pulse duration is extremely small. Between two pulses, the detuning $\Delta(t) = \Delta_0$ keeps a constant value. The quantum Langevin equations can be obtained as

$$\dot{a} = [-\frac{\kappa}{2} + i\Delta(t)]a + iga(b^\dagger + b) - i\Omega + a_{\text{in}}, \quad (\text{A3})$$

$$\dot{b} = (-\frac{\gamma}{2} - i\omega_m)b + iga^\dagger a + b_{\text{in}}, \quad (\text{A4})$$

where κ (γ) is the decay rate of the optical (mechanical) mode, and a_{in} and b_{in} are the corresponding noise operators. Here we employ the linearization process by replacing optical and mechanical operators with their average values and fluctuations, i.e. $a \rightarrow a + \alpha$ and $b \rightarrow b + \beta$, where the average values satisfy

$$\dot{\alpha} = [-\frac{\kappa}{2} + i\Delta(t)]\alpha + ig\alpha(\beta^* + \beta) - i\Omega, \quad (\text{A5})$$

$$\dot{\beta} = (-\frac{\gamma}{2} - i\omega_m)\beta + ig|\alpha|^2. \quad (\text{A6})$$

Noted that α and β given by Eq. (A5) and (A6) are also time-dependent as the detuning is changed periodically. However, the time-dependent effect can be neglected as the pulse duration is small. And in principle, we can obtain constant solutions if the driving strength is also changed periodically. Then the quantum Langevin equations become

$$\dot{a} = [-\frac{\kappa}{2} + i\Delta'(t)]a + iga(b^\dagger + b) + iG(b^\dagger + b) + a_{\text{in}}, \quad (\text{A7})$$

$$\dot{b} = (-\frac{\gamma}{2} - i\omega_m)b + iga^\dagger a + i(Ga^\dagger + G^*a) + b_{\text{in}}, \quad (\text{A8})$$

where $\Delta'(t) = \Delta(t) - g(\beta + \beta^*)$ is the effective detuning and $G = g\alpha$ is the enhanced optomechanical coupling strength (We assume G is a constant.). Considering small single-photon coupling strength and strong optical driving, the nonlinear terms $iga(b^\dagger + b)$ and $iga^\dagger a$ in Eq. (A7) and (A8) can be neglected and the linearized system Hamiltonian becomes

$$H_L = -\Delta'(t)a^\dagger a + \omega_m b^\dagger b + (Ga^\dagger + G^*a)(b + b^\dagger). \quad (\text{A9})$$

Appendix B: Baker-Campbell-Hausdorff formula and effective Hamiltonian

In the Schrödinger picture, the evolution of the optomechanical system is described by the operator $\mathcal{U}(t) = e^{-i\int H_L dt}$. Between two pulses, the effective detuning $\Delta'(t) = \Delta_0 - g(\beta^* + \beta) \equiv \Delta'_0$ keeps a small and constant value. But during the rotating pulses, the effective detuning was rapidly enlarged to a huge value (in a time scale slower than the round trip time but much faster than t_0). In this case, the evolution of mechanical mode as well as the optomechanical coupling, i.e. the second and third term in Eq. (A9) can be neglected. The system is well described by the rotating operator $R(\theta_j) = e^{i\theta_j a^\dagger a}$, where $\theta_j = \int_{j t_0}^{j t_0 + \delta t} \Delta(\tau) d\tau$, $j = 0, 1, 2, \dots$ is the rotating angle during every pulse and $\theta_j = \phi, \pm\pi - \phi, \phi, \pm\pi - \phi, \dots$ in our pulse structure. We define four pulses as a period because the total phase (angle) is 2π after a four-pulse period $T = 4t_0$. The evolution operator in a period can be described by

$$\mathcal{U}(T) = [R(\pi - \phi)U(t_0)R(\phi)U(t_0)]^2, \quad (\text{B1})$$

where $U(t_0) = e^{-iH_L t_0}$ for $\Delta'(t) = \Delta'_0$. With the relation $R(\theta_1 + \theta_2) = R(\theta_1)R(\theta_2)$, $R(\theta)aR(-\theta) = ae^{-i\theta}$, the left of Eq. (B1) can be separated into four parts as

$$R(\pi - \phi)U(t_0)R(\phi - \pi) = \text{Exp}\{-it_0(-\Delta'_0 a^\dagger a + \omega_m b^\dagger b - (Ga^\dagger e^{-i\phi} + G^* a e^{i\phi})(b + b^\dagger))\}, \quad (\text{B2})$$

$$R(\pi)U(t_0)R(-\pi) = \text{Exp}\{-it_0(-\Delta'_0 a^\dagger a + \omega_m b^\dagger b - (Ga^\dagger + G^* a)(b + b^\dagger))\}, \quad (\text{B3})$$

$$R(-\phi)U(t_0)R(\phi) = \text{Exp}\{-it_0(-\Delta'_0 a^\dagger a + \omega_m b^\dagger b + (Ga^\dagger e^{-i\phi} + G^* a e^{i\phi})(b + b^\dagger))\}, \quad (\text{B4})$$

$$U(t_0) = \text{Exp}\{-it_0(-\Delta'_0 a^\dagger a + \omega_m b^\dagger b + (Ga^\dagger + G^* a)(b + b^\dagger))\}, \quad (\text{B5})$$

where we have also used the identity $R(\pi) = R(-\pi)$, because $R(2\pi)$ is trivial in the evolution. In the approximation that the pulse interval satisfies $t_0 \ll \omega_m^{-1}$, we can use the two-order Baker-Campbell-Hausdorff formula $e^{X+Y} \approx X + Y + \frac{1}{2}[X, Y]$. Then a Hamiltonian that sat-

isfied $\mathcal{U}(T) = e^{-iH_0 T}$ can be obtained as $H_0 = H_{\text{eff}} + H'$, where

$$H_{\text{eff}} = \omega_m b^\dagger b + \sigma(b + b^\dagger)^2, \quad (\text{B6})$$

$$\sigma = \frac{1}{2}|G|^2 t_0 \sin\phi, \quad (\text{B7})$$

and $H' = -\Delta'_0 a^\dagger a + \Delta'_0 (\mu a^\dagger + \mu^* a)(b + b^\dagger) + \omega_m (\mu a^\dagger - \mu^* a)(b - b^\dagger)$, $\mu = \frac{1}{4} G t_0 (1 + e^{i\phi})$. The second term in the left of Eq. (B6) is what we are interested for generating mechanical squeezing. And fortunately, the last two terms in H' can be neglected in the condition that $|G \sin\phi| \gg |\Delta'_0|, \omega_m$ and $|\mu| \ll 1$. It means that our pulsed scheme can equivalently transpose the optomechanical coupling into a constant modulation of the potential of the mechanical oscillator. The mechanical mode will dynamically evolve into a squeezed state. For $\sigma > -\frac{\omega_m}{4}$, Eq. (B6) can be rewritten in the classical view as

$$H_{\text{eff}} = \omega_s \left(\sqrt{\frac{\omega_m + 4\sigma}{\omega_m}} X_M^2 + \sqrt{\frac{\omega_m}{\omega_m + 4\sigma}} P_M^2 \right), \quad (\text{B8})$$

where $X_M = b^\dagger + b$, $P_M = i(b^\dagger - b)$ are mechanical quadratures and ω_s is the effective frequency as

$$\omega_s = \sqrt{\omega_m(\omega_m + 4\sigma)}. \quad (\text{B9})$$

For $\sigma < -0.25\omega_m$, the mechanical mode evolves exponentially with an exponential gain as

$$\epsilon = \sqrt{-\omega_m(\omega_m + 4\sigma)}. \quad (\text{B10})$$

Appendix C: Quantum master equations

In order to numerically analyze the mechanical squeezing, we write down the quantum master equations as

$$\begin{aligned} \dot{\rho} = & i[\rho, H_L] + \frac{\kappa}{2}(2a\rho a^\dagger - a^\dagger a\rho - \rho a^\dagger a) \\ & + \frac{\gamma}{2}(n_{\text{th}} + 1)(2b\rho b^\dagger - b^\dagger b\rho - \rho b^\dagger b) \\ & + \frac{\gamma}{2}n_{\text{th}}(2b^\dagger \rho b - b b^\dagger \rho - \rho b b^\dagger). \end{aligned} \quad (\text{C1})$$

$$\begin{aligned} \langle b^\dagger b \rangle(t) = & -\frac{4\sigma^2}{\omega_s^2} \left\{ a + e^{-\gamma t} \left[(n_{\text{th}} - a) \cos(2\omega_s t) + \frac{\gamma}{2\omega_s} (n_m - a) \sin(2\omega_s t) \right] \right\} \\ & + \frac{(\omega_m + 2\sigma)^2}{\omega_s^2} [n_m + (n_{\text{th}} - n_m)e^{-\gamma t}], \end{aligned} \quad (\text{C5})$$

$$\begin{aligned} \text{Re}\langle b^2 \rangle(t) = & \frac{2\sigma(\omega_m + 2\sigma)}{\omega_s^2} \\ & \left\{ a - n_m + e^{-\gamma t} \left[(n_{\text{th}} - a) \cos(2\omega_s t) + \frac{\gamma}{2\omega_s} (n_m - a) \sin(2\omega_s t) + n_m - n_{\text{th}} \right] \right\}, \end{aligned} \quad (\text{C6})$$

$$\text{Im}\langle b^2 \rangle(t) = -\frac{2\sigma}{\omega_s} \left\{ b \left[1 - e^{-\gamma t} \left(\cos(2\omega_s t) + \frac{\gamma}{2\omega_s} \sin(2\omega_s t) \right) \right] + e^{-\gamma t} \left(n_{\text{th}} + \frac{1}{2} \right) \sin(2\omega_s t) \right\}, \quad (\text{C7})$$

with n_{th} the initial phonon number and

$$a = \text{Re} \left(\frac{\gamma n_m + i\omega_s}{\gamma - 2i\omega_s} \right), \quad b = \text{Im} \left(\frac{\gamma n_m + i\omega_s}{\gamma - 2i\omega_s} \right). \quad (\text{C8})$$

It's useless and difficult to calculate the whole density matrix. We are only concerned about the evolution of quadrature variances, which can be obtained from the average values of the second-order operators, $\langle a^\dagger a \rangle$, $\langle b^\dagger b \rangle$, $\langle ab^\dagger \rangle$, $\langle ab \rangle$, $\langle a^2 \rangle$, $\langle b^2 \rangle$. They are determined by a system of linear equations as

$$\partial_t \langle \hat{o}_i \hat{o}_j \rangle = \text{Tr}(\hat{\rho} \dot{\hat{o}}_i \hat{o}_j) = \sum_{k,l} \eta_{k,l} \langle \hat{o}_k \hat{o}_l \rangle, \quad (\text{C2})$$

where $\hat{o}_{i,j,k}$ are operators $a, b, a^\dagger, b^\dagger$ and $\eta_{k,l}$ can be obtained from Eq. (C1). Analytical results can be obtained by replacing H_L with H_{eff} in Eq. (C1).

Analytical results can be obtained by replacing H_L with H_{eff} in Eq. (C1). Then the system is governed by

$$\frac{d}{dt} \langle b^\dagger b \rangle = -\gamma \langle b^\dagger b \rangle - 2i\sigma \langle b^{\dagger 2} \rangle + 2i\sigma \langle b^2 \rangle + \gamma n_m, \quad (\text{C3})$$

$$\frac{d}{dt} \langle b^2 \rangle = (-\gamma - 2i\omega_m - 4i\sigma) \langle b^2 \rangle - 2i\sigma (\langle b^\dagger b \rangle + \langle b b^\dagger \rangle), \quad (\text{C4})$$

where n_m is the thermal occupation number of the environment, and the optical mode is neglected. For $\sigma > -\frac{\omega_m}{4}$, the exact solution is

The quadrature variances satisfy $\delta X_M^2 = 1 + 2(\langle b^\dagger b \rangle + \langle b^2 \rangle)$ and $\delta P_M^2 = 1 + 2(\langle b^\dagger b \rangle - \langle b^2 \rangle)$. The variance of squeezed quadrature Y_M satisfies $\delta Y_M^2 = 1 + 2(\langle b^\dagger b \rangle - |\langle b^2 \rangle|)$. In the short-time approximation $\omega_m t_0 \ll 1$ and $\gamma n_m \ll 1$, the evolution of quadrature variances can be obtained as

$$\delta P_M^2 = (1 + 2n_{\text{th}}) \left[1 + \frac{2\sigma}{\omega_m} (1 - \cos 2\omega_s t) \right], \quad (\text{C9})$$

$$\delta X_M^2 = (1 + 2n_{\text{th}}) \left[1 - \frac{2\sigma}{\omega_m + 4\sigma} (1 - \cos 2\omega_s t) \right], \quad (\text{C10})$$

$$\delta Y_M^2 = 1 + 2 \left\{ n_{\text{th}} + \frac{2}{\omega_s^2} (2n_{\text{th}} + 1) \sin^2(\omega_s t) \left[2\sigma^2 - |\sigma| \sqrt{(\omega_m + 2\sigma)^2 + \omega_s^2 \cot^2(\omega_s t)} \right] \right\}. \quad (\text{C11})$$

Then the squeezing limit is given by (corresponding to Eq. (9) in the main text)

$$(\delta Y_M^2)_{\min} = \begin{cases} (1 + 2n_{\text{th}}) \frac{\omega_m + 4\sigma}{\omega_m}, & -\frac{\omega_m}{4} < \sigma < 0 \\ (1 + 2n_{\text{th}}) \frac{\omega_m}{\omega_m + 4\sigma}, & \sigma > 0 \end{cases} \quad (\text{C12})$$

which is approached at $\omega_s t = n\pi + \pi/2$, $n = 0, 1, 2, \dots$. There is maximal squeezing degree at the first point of time $t_m = \frac{\pi}{2\omega_s}$, if considering the influence of the decay rates. In the maximally squeezed state, quadrature P_M is squeezed for $-\frac{\omega_m}{4} < \sigma < 0$ while X_M is squeezed for $\sigma > 0$.

By contrast in the long-time approximation, the steady value of quadrature variances reads

$$\delta P_M^2 = (1 + 2n_m) \left(1 + \frac{2\sigma(\omega_m + 4\sigma)}{\gamma^2/4 + \omega_s^2} \right), \quad (\text{C13})$$

$$\delta X_M^2 = (1 + 2n_m) \left(1 - \frac{2\sigma\omega_m}{\gamma^2/4 + \omega_s^2} \right). \quad (\text{C14})$$

The squeezing degree can't suppress the 3dB limit in the steady state.

And for $\sigma = -\frac{\omega_m}{4}$, the exact solution is

$$\langle b^\dagger b \rangle(t) = \frac{\omega_m^2}{2\gamma^2} [\gamma^2 t^2 (n_{\text{th}} - n_m) - (\gamma t + 1)(2n_m + 1)] e^{-\gamma t} + (n_{\text{th}} - n_m) e^{-\gamma t} + \frac{\omega_m^2}{2\gamma^2} (2n_m + 1) + n_m, \quad (\text{C15})$$

$$\text{Re}\langle b^2 \rangle(t) = \frac{\omega_m^2}{2\gamma^2} [\gamma^2 t^2 (n_{\text{th}} - n_m) - (\gamma t + 1)(2n_m + 1)] e^{-\gamma t} + \frac{\omega_m^2}{2\gamma^2} (2n_m + 1), \quad (\text{C16})$$

$$\text{Im}\langle b^2 \rangle(t) = \frac{\omega_m}{2\gamma} [2\gamma t (n_{\text{th}} - n_m) - (2n_m + 1)] e^{-\gamma t} + \frac{\omega_m}{2\gamma} (2n_m + 1). \quad (\text{C17})$$

Letting $\gamma = 0$, we obtained

$$\delta Y_M^2(t) = (1 + 2n_{\text{th}}) \left[1 - \frac{\omega_m^2 t^2}{2} \left(\sqrt{1 + \frac{4}{\omega_m^2 t^2}} - 1 \right) \right]. \quad (\text{C18})$$

For $\sigma < -\frac{\omega_m}{4}$ and $\gamma \neq \epsilon$, the exact solution is

$$\begin{aligned} \langle b^\dagger b \rangle(t) &= [-\omega_0^2 + 8\sigma^2 (e^{2\epsilon t} + e^{-2\epsilon t})] \frac{n_{\text{th}}}{4\epsilon^2} e^{-\gamma t} \\ &+ \frac{\omega_0^2 + \gamma^2}{\gamma^2 - 4\epsilon^2} n_m - \left[-\omega_0^2 + 8\sigma^2 \left(\frac{\gamma}{\gamma - 2\epsilon} e^{2\epsilon t} + \frac{\gamma}{\gamma + 2\epsilon} e^{-2\epsilon t} \right) \right] \frac{n_m}{4\epsilon^2} e^{-\gamma t} \\ &+ \frac{8\sigma^2}{\gamma^2 - 4\epsilon^2} - \left[\frac{1}{\gamma - 2\epsilon} e^{2\epsilon t} - \frac{1}{\gamma + 2\epsilon} e^{-2\epsilon t} \right] \frac{2\sigma^2}{\epsilon} e^{-\gamma t}, \end{aligned} \quad (\text{C19})$$

$$\begin{aligned}
\text{Re}(b^2)(t) &= \left[1 - \frac{1}{2}(e^{2\epsilon t} + e^{-2\epsilon t})\right] \frac{\sigma\omega_0 n_{\text{th}}}{\epsilon^2} e^{-\gamma t} \\
&\quad - \frac{4\sigma\omega_0}{\gamma^2 - 4\epsilon^2} n_m - \left[1 - \left(\frac{\gamma}{\gamma - 2\epsilon} e^{2\epsilon t} + \frac{\gamma}{\gamma + 2\epsilon} e^{-2\epsilon t}\right)\right] \frac{\sigma\omega_0 n_m}{\epsilon^2} e^{-\gamma t} \\
&\quad - \frac{2\sigma\omega_0}{\gamma^2 - 4\epsilon^2} + \left[\frac{1}{\gamma - 2\epsilon} e^{2\epsilon t} - \frac{1}{\gamma + 2\epsilon} e^{-2\epsilon t}\right] \frac{\omega_0\sigma}{2\epsilon} e^{-\gamma t},
\end{aligned} \tag{C20}$$

$$\begin{aligned}
\text{Im}(b^2)(t) &= -(e^{2\epsilon t} - e^{-2\epsilon t}) \frac{\sigma n_{\text{th}}}{\epsilon} e^{-\gamma t} \\
&\quad - \frac{4\sigma\gamma}{\gamma^2 - 4\epsilon^2} n_m + \left(\frac{1}{\gamma - 2\epsilon} e^{2\epsilon t} - \frac{1}{\gamma + 2\epsilon} e^{-2\epsilon t}\right) \frac{\sigma\gamma n_m}{\epsilon} e^{-\gamma t} \\
&\quad - \frac{2\gamma\sigma}{\gamma^2 - 4\epsilon^2} + \left[\frac{1}{\gamma - 2\epsilon} e^{2\epsilon t} + \frac{1}{\gamma + 2\epsilon} e^{-2\epsilon t}\right] \sigma e^{-\gamma t}.
\end{aligned} \tag{C21}$$

Letting $\gamma = 0$, we obtained

$$\delta Y_M^2(t) = (1 + 2n_{\text{th}}) \left\{ 1 - \frac{2\sigma^2}{\epsilon^2} (1 - e^{-2\epsilon t}) \left[\sqrt{(e^{2\epsilon t} - 1)^2 + e^{2\epsilon t} \frac{\epsilon^2}{\sigma^2}} - (e^{2\epsilon t} - 1) \right] \right\}. \tag{C22}$$

Appendix D: Wigner Function

In this section, we will provide the detailed calculation of the Wigner function where we can see the squeezing dynamics and performance visually. The initial states of optical and mechanical modes are both thermal states, the Wigner functions of which can be written as

$$W(q, p) = \frac{1}{\pi(\langle n \rangle + 1/2)} e^{-(q^2 + p^2)/(\langle n \rangle + 1/2)}, \tag{D1}$$

where $\langle n \rangle$ is the average occupation number. In the optomechanical system, it's more useful to calculate the Wigner function in total phase space including both optical and mechanical quadratures, which is

$$W_{\text{total}}(X_L, P_L, X_M, P_M, t) = W_L(X_L, P_L, t) \times W_M(X_M, P_M, t). \tag{D2}$$

Here $W_L(X_L, P_L, t)$ and $W_M(X_M, P_M, t)$ are the Wigner functions of the optical and mechanical modes, which can be obtained from the integral of Eq. (D2) over the other phase space. The Wigner function of the initial state is

$$W_{\text{total}}(\mathbf{X}, 0) = \left(\frac{1}{\pi(n_{\text{th}} + 1/2)} \right)^2 e^{-\mathbf{X}^T \mathbf{X}/(n_{\text{th}} + 1/2)}, \tag{D3}$$

where we have defined $\mathbf{X} = (X_L, P_L, X_M, P_M)^T$ and n_{th} is the initial phonon number. The evolution of quadrature "vector" \mathbf{X} is described by

$$\mathbf{X}(t) = \mathcal{U}(t)\mathbf{X}(0) \equiv \mathcal{A}\mathbf{X}(0), \tag{D4}$$

where $\mathcal{U}(t)$ is the evolution operator and \mathcal{A} is a matrix that denotes the linear evolution of $\mathbf{X}(t)$. Then the time

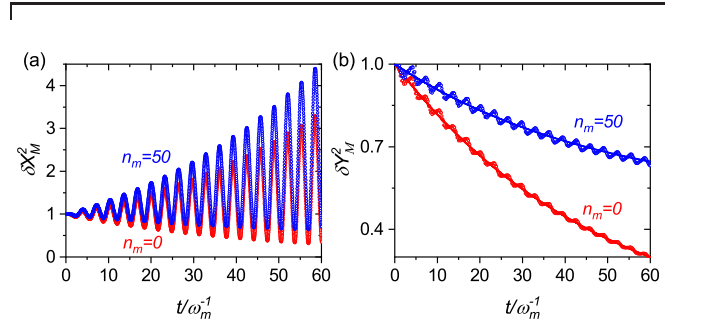


FIG. 5. (a),(b) The evolution of variances of mechanical quadratures X_M (a) and Y_M (b) for $n_m = 0$ in red and $n_m = 50$ in blue. In panel (b), the theoretical evolution (solid line) given by Eq. (E2) agrees well with the numerical results (open circles) based on the driving strength modulated as Eq. (E1).

evolution of the total Wigner function can be obtained as

$$W_{\text{total}}(\mathbf{X}, t) = \left(\frac{1}{\pi(n_{\text{th}} + 1/2)} \right)^2 e^{-(\mathcal{A}\mathbf{X})^T \mathcal{A}\mathbf{X}/(n_{\text{th}} + 1/2)}. \tag{D5}$$

And the optical and mechanical Wigner functions are given by

$$W_L(X_L, P_L, t) = \int_{-\infty}^{\infty} dX_M \int_{-\infty}^{\infty} dP_M W_{\text{total}}(\mathbf{X}, t), \tag{D6}$$

$$W_M(X_M, P_M, t) = \int_{-\infty}^{\infty} dX_L \int_{-\infty}^{\infty} dP_L W_{\text{total}}(\mathbf{X}, t). \tag{D7}$$

Appendix E: Parametric resonance

Another efficient way to generate mechanical squeezing in the optomechanical system is to consider the mechanical mode as a parametric oscillator, which can also be used in our model. Parametric resonance occurs when the external driving strength is modulated as

$$\Omega(t) = \Omega_0 \sin(\omega_s t), \quad (\text{E1})$$

with Ω_0 being a constant and ω_s given by Eq. (B9) where we find numerically $G \approx 0.45g\Omega_0 t_0$. Noted that the average values α and β are time-dependent but can also be calculated by master equations. In Fig. 5, we plot the evolution of mechanical quadrature variances in the parametric resonance case. The squeezing performance is limited by the thermal occupation number n_m . The numerical results agree well with the adiabatic theory given by Jieqiao Liao *et al* [6]. Starting from the vacuum state, the evolution of squeezed quadrature can be described by

$$\delta Y_M^2(t) \approx e^{-(\gamma+\xi_0)t} + \frac{\gamma(2n_m+1)}{\gamma+\xi_0}(1 - e^{-(\gamma+\xi_0)t}), \quad (\text{E2})$$

where $\xi_0 = |\omega_s - \omega_m|$ describes the parametric gain in parametric resonance. Unlike the large-detuning system in Ref. [6], ξ_0 can be arbitrarily large with appropriate parameters, i.e. $t_0 \rightarrow 0$, $G \rightarrow \infty$ and $\phi = \pi/2$, which also has potential in the generation of strong mechanical squeezing in the steady state [10].

Appendix F: Discussion about the detuning-switched driving

To obtain the mechanical squeezing with detuning-switched driving, an important requirement is that the cavity must oscillate following the laser driving, i.e. the cavity must react to the large detuning. We discuss this requirement from two different aspects.

First, we consider a general classical Langevin equation describing a single-mode cavity

$$\dot{a}(t) = (i\omega_0 - \kappa/2)a(t) + F(t), \quad (\text{F1})$$

where $a(t)$ is the classical cavity field, ω_0 is the cavity resonance frequency, κ is the cavity decay rate and $F(t) = Ae^{i\omega t}$ is a harmonic drive. The solution after applying the drive ($t > t_0$) is given by

$$a(t) = e^{(i\omega_0 - \kappa/2)(t-t_0)} \left[a(t_0) - \frac{Ae^{i\omega t_0}}{i(\omega - \omega_0) + \kappa/2} \right] + e^{i\omega(t-t_0)} \frac{Ae^{i\omega t_0}}{i(\omega - \omega_0) + \kappa/2}. \quad (\text{F2})$$

Initially the cavity is driven by a laser $F_1(t) = A_1 e^{i\omega_1 t}$ near the resonance $\omega_1 \approx \omega_0$, the cavity field will reach a steady-state amplitude $\left| \frac{A_1}{i(\omega_1 - \omega_0) - \kappa/2} \right|$. Assume at $t = 0$

we suddenly increase the detuning to a large value with a driving $F_2 = A_2 e^{i\omega_2 t}$ and an initial condition $a(0) = \frac{A_1}{i(\omega_1 - \omega_0) + \kappa/2}$, the following evolution will be

$$a(t) = e^{(i\omega_0 - \kappa/2)t} \left[\frac{A_1}{i(\omega_1 - \omega_0) + \kappa/2} - \frac{A_2}{i(\omega_2 - \omega_0) + \kappa/2} \right] + e^{i\omega_2 t} \frac{A_2}{i(\omega_2 - \omega_0) + \kappa/2}. \quad (\text{F3})$$

Consequently, to make the cavity field change from frequency ω_1 to ω_2 and acquire the rotating phase we wanted, the driving laser should satisfy

$$\frac{A_1}{i(\omega_1 - \omega_0) + \kappa/2} = \frac{A_2}{i(\omega_2 - \omega_0) + \kappa/2}. \quad (\text{F4})$$

It means that when we increase the detuning of the laser, we also need to increase the power of the laser accordingly. Then in the frame with laser frequency, although the optomechanical coupling strength remains constant, the cavity field will rotate and acquire a phase; and in the frame with cavity resonance frequency, the cavity field does not rotate but the optomechanical coupling strength will rotate, leading to a new kind of squeezing effect in the mechanical oscillator.

Second, an optical cavity differs from a cavity described by the single-mode Langevin equation. An optical cavity is not a point object and can not react instantaneously to the sudden change of a driving laser, as everything propagates at the speed of light. This propagation effect is not captured by the Langevin equation, which only provides the amplitude-phase degrees of freedom.

The finite propagation speed of the light can be captured if multiple azimuthal modes are involved. The frequency domain picture of this system is periodic Lorentzian response functions spaced by the FSR. The inverted time domain response is a periodic near-delta function spaced by the round-trip time, which captures the round-trip dynamics of the input pulse bouncing back and forth between the two mirrors. Therefore, when there is a sudden change of the input field, instead of immediately forming a new oscillation frequency inside the cavity, it could well be that this sudden change results in some localized pulse structure in space and time, and bounce back and forth inside the cavity for a very long time until the cavity decays to a new equilibrium state. It is far away from what we want in the squeezing mechanism, where we want an immediate switch of the oscillation frequency. Therefore the cavity field needs to switch to a new equilibrium instantly.

The frequency domain picture provides some insights on how to avoid such a scenario. When there is a sudden switch of the input laser, this step-like change contains extremely broad frequency components, and can excite multiple optical modes spanning many FSRs. Such an excitation in the time domain is the resulting localized intracavity structure that requires a very long time to

reach a new equilibrium. Therefore, the laser frequency (also amplitude) switching should not be arbitrarily fast in the sense that other azimuthal optical modes should not be excited. The switching needs to be slower than the FSR, or the round trip time of the cavity, so the cavity field can adiabatically reach a new equilibrium during the switching. Therefore, the requirement on the laser switching scheme is that it should not be faster than the round trip time, but should be a lot faster than all the other time scales in the experiment, e.g. the inverse of G , κ , ω_m , etc.

Realistically, this issue might not pose any problem for optical implementations, since the FSR in optical domains is usually GHz range for well-established platforms. However, it could be a realistic concern for microwave platforms where switching of the microwave fields can be really fast, faster than the microwave frequency, and the frequency spacing to higher order modes (FSR).

Appendix G: Experimental realization

The optomechanical system we considered is in the strong coupling regime ($G > \omega_m$), and the squeezing mechanism requires the optical cavity can respond quickly to the detuning of the driving laser, which limits that the cavity decay rate can not be too small. Such a condition is possible with an experimental setup of a three-dimensional microwave cavity [37]. The mechanical frequency is around $\omega_m \approx 9.696\text{MHz}$, the single-photon optomechanical coupling strength is $g \approx 167\text{Hz}$, and the cavity decay rate is $\kappa \approx 1\text{MHz}$. To enter the strong coupling regime, the average intra-cavity photon number should exceed $(\omega_m/g)^2 \approx 3.37 \times 10^9$. For a detuned cavity, the average intra-cavity photon number is given by

$$n_{\text{cav}} = \frac{P}{\hbar\omega_L} \frac{\kappa}{(\kappa/2)^2 + \Delta^2}, \quad (\text{G1})$$

where P is the power of the driving laser. In our model, the detuning is switched to a large value periodically. So the intra-cavity photon number is limited by the detunings instead of the cavity decay rate. For typical laser detuning $\Delta = 10\omega_m$, the laser power should exceed $136\mu\text{W}$ (at frequency 6.5GHz). Consequently, the squeezing mechanism proposed here is realizable with existing platforms, and the mechanical squeezing can be observed through an additional probe beam.

-
- [1] V. B. Braginsky, Y. I. Vorontsov, and K. S. Thorne, Quantum Nondemolition Measurements, *Science* **209**, 547 (1980).
- [2] S. C. Burd, R. Srinivas, J. J. Bollinger, A. C. Wilson, D. J. Wineland, D. Leibfried, D. H. Slichter, and D. T. C. Allcock, Quantum amplification of mechanical oscillator motion, *Science* **364**, 1163 (2019).
- [3] L. S. Brown, Squeezed states and quantum-mechanical parametric amplification, *Phys. Rev. A* **36**, 2463 (1987).
- [4] D. Rugar and P. Grütter, Mechanical parametric amplification and thermomechanical noise squeezing, *Phys. Rev. Lett.* **67**, 699 (1991).
- [5] M. Zalalutdinov, A. Olkhovets, A. Zehnder, B. Ilic, D. Czaplewski, H. Craighead, and J. Parpia, Optically pumped parametric amplification for micromechanical oscillators, *Appl. Phys. Lett.* **78**, 3142 (2001).
- [6] J.-Q. Liao and C. K. Law, Parametric generation of quadrature squeezing of mirrors in cavity optomechanics, *Phys. Rev. A* **83**, 033820 (2011).
- [7] A. Pontin, M. Bonaldi, A. Borrielli, F. S. Cataliotti, F. Marino, G. A. Prodi, E. Serra, and F. Marin, Squeezing a thermal mechanical oscillator by stabilized parametric effect on the optical spring, *Phys. Rev. Lett.* **112**, 023601 (2014).
- [8] X. You, Z. Li, and Y. Li, Strong quantum squeezing of mechanical resonator via parametric amplification and coherent feedback, *Phys. Rev. A* **96**, 063811 (2017).
- [9] S. Sonar, V. Fedoseev, M. J. Weaver, F. Luna, E. Vlieg, H. van der Meer, D. Bouwmeester, and W. Löffler, Strong thermomechanical squeezing in a far-detuned membrane-in-the-middle system, *Phys. Rev. A* **98**, 013804 (2018).
- [10] A. Szorkovszky, A. C. Doherty, G. I. Harris, and W. P. Bowen, Mechanical squeezing via parametric amplification and weak measurement, *Phys. Rev. Lett.* **107**, 213603 (2011).
- [11] A. Szorkovszky, G. A. Brawley, A. C. Doherty, and W. P. Bowen, Strong thermomechanical squeezing via weak measurement, *Phys. Rev. Lett.* **110**, 184301 (2013).
- [12] A. Vinante and P. Falferi, Feedback-enhanced parametric squeezing of mechanical motion, *Phys. Rev. Lett.* **111**, 207203 (2013).
- [13] A. A. Clerk, F. Marquardt, and K. Jacobs, Back-action evasion and squeezing of a mechanical resonator using a cavity detector, *New J. Phys.* **10**, 095010 (2008).
- [14] J. B. Hertzberg, T. Rocheleau, T. Ndukum, M. Savva, A. A. Clerk, and K. C. Schwab, Back-action-evading measurements of nanomechanical motion, *Nat. Phys.* **6**, 213 (2010).
- [15] F. Lecocq, J. B. Clark, R. W. Simmonds, J. Aumentado, and J. D. Teufel, Quantum nondemolition measurement of a nonclassical state of a massive object, *Phys. Rev. X* **5**, 041037 (2015).
- [16] E. E. Wollman, C. U. Lei, A. J. Weinstein, J. Suh, A. Kronwald, F. Marquardt, A. A. Clerk, and K. C. Schwab, Quantum squeezing of motion in a mechanical

- resonator, *Science* **349**, 952 (2015).
- [17] M. Brunelli, D. Malz, and A. Nunnenkamp, Conditional dynamics of optomechanical two-tone backaction-evading measurements, *Phys. Rev. Lett.* **123**, 093602 (2019).
- [18] C. Meng, G. A. Brawley, J. S. Bennett, M. R. Vanner, and W. P. Bowen, Mechanical squeezing via fast continuous measurement, *Phys. Rev. Lett.* **125**, 043604 (2020).
- [19] A. C. Doherty and K. Jacobs, Feedback control of quantum systems using continuous state estimation, *Phys. Rev. A* **60**, 2700 (1999).
- [20] A. Kronwald, F. Marquardt, and A. A. Clerk, Arbitrarily large steady-state bosonic squeezing via dissipation, *Phys. Rev. A* **88**, 063833 (2013).
- [21] J.-M. Pirkkalainen, E. Damskäg, M. Brandt, F. Massel, and M. A. Sillanpää, Squeezing of quantum noise of motion in a micromechanical resonator, *Phys. Rev. Lett.* **115**, 243601 (2015).
- [22] H.-Y. Fan and H. R. Zaidi, Squeezing and frequency jump of a harmonic oscillator, *Phys. Rev. A* **37**, 2985 (1988).
- [23] G. S. Agarwal and S. A. Kumar, Exact quantum-statistical dynamics of an oscillator with time-dependent frequency and generation of nonclassical states, *Phys. Rev. Lett.* **67**, 3665 (1991).
- [24] M. Rashid, T. Tufarelli, J. Bateman, J. Vovrosh, D. Hempston, M. S. Kim, and H. Ulbricht, Experimental realization of a thermal squeezed state of levitated optomechanics, *Phys. Rev. Lett.* **117**, 273601 (2016).
- [25] M. Xin, W. S. Leong, Z. Chen, Y. Wang, and S.-Y. Lan, Rapid Quantum Squeezing by Jumping the Harmonic Oscillator Frequency, *Phys. Rev. Lett.* **127**, 183602 (2021).
- [26] A. Mari and J. Eisert, Gently modulating optomechanical systems, *Phys. Rev. Lett.* **103**, 213603 (2009).
- [27] H. Tan and H. Zhan, Strong mechanical squeezing and optomechanical steering via continuous monitoring in optomechanical systems, *Phys. Rev. A* **100**, 023843 (2019).
- [28] B. Xiong, X. Li, S.-L. Chao, Z. Yang, W.-Z. Zhang, W. Zhang, and L. Zhou, Strong mechanical squeezing in an optomechanical system based on Lyapunov control, *Photonics Res.* **8**, 151 (2020).
- [29] R. Ruskov, K. Schwab, and A. N. Korotkov, Squeezing of a nanomechanical resonator by quantum nondemolition measurement and feedback, *Phys. Rev. B* **71**, 235407 (2005).
- [30] M. R. Vanner, I. Pikovski, G. D. Cole, M. S. Kim, C. Brukner, K. Hammerer, G. J. Milburn, and M. Aspelmeyer, Pulsed quantum optomechanics, *Proc. Natl. Acad. Sci. U. S. A.* **108**, 16182 (2011).
- [31] K. Kustura, C. Gonzalez-Ballester, A. d. I. R. Sommer, N. Meyer, R. Quidant, and O. Romero-Isart, Mechanical Squeezing via Unstable Dynamics in a Microcavity, *Phys. Rev. Lett.* **128**, 143601 (2022).
- [32] M. R. Vanner, J. Hofer, G. D. Cole, and M. Aspelmeyer, Cooling-by-measurement and mechanical state tomography via pulsed optomechanics, *Nat. Commun.* **4**, 2295 (2013).
- [33] J. T. Muhonen, G. R. La Gala, R. Leijssen, and E. Verhagen, State preparation and tomography of a nanomechanical resonator with fast light pulses, *Phys. Rev. Lett.* **123**, 113601 (2019).
- [34] K. E. Khosla, M. R. Vanner, W. P. Bowen, and G. J. Milburn, Quantum state preparation of a mechanical resonator using an optomechanical geometric phase, *New J. Phys.* **15**, 043025 (2013).
- [35] J. S. Bennett and W. P. Bowen, Rapid mechanical squeezing with pulsed optomechanics, *New J. Phys.* **20**, 113016 (2018).
- [36] L. Xin, M. S. Chapman, and T. A. B. Kennedy, Fast Generation of Time-Stationary Spin-1 Squeezed States by Nonadiabatic Control, *PRX Quantum* **3**, 010328 (2022).
- [37] G. A. Peterson, S. Kotler, F. Lecocq, K. Cicak, X. Y. Jin, R. W. Simmonds, J. Aumentado, and J. D. Teufel, Ultrastrong Parametric Coupling between a Superconducting Cavity and a Mechanical Resonator, *Phys. Rev. Lett.* **123**, 247701 (2019).